

Supplementary Materials for

Atomically thin gallium layers from solid-melt exfoliation

Vidya Kochat, Atanu Samanta, Yuan Zhang, Sanjit Bhowmick, Praveena Manimunda, Syed Asif S. Asif, Anthony S. Stender, Robert Vajtai, Abhishek K. Singh, Chandra S. Tiwary, Pulickel M. Ajayan

Published 9 March 2018, *Sci. Adv.* **4**, e1701373 (2018)

DOI: 10.1126/sciadv.1701373

This PDF file includes:

- section S1. Bulk gallium structural analysis
- section S2. Stability of gallenene sheets
- section S3. Effect of thickness on the band structure of gallenene
- section S4. Stamping technique of solid-melt exfoliation
- section S5. AFM analysis of Ga films
- section S6. Contact angle measurements
- section S7. Substrate effects on gallenene
- section S8. Absorption measurements on gallenene
- section S9. XPS measurements on Ga/MoS₂ heterostructures
- section S10. Structural stability of Ga/MoS₂ heterostructures
- section S11. Thermal conductivity of gallenene
- section S12. Defects in gallenene
- section S13. Polymorphism in gallenene
- section S14. Exfoliation of ultrathin Sn sheets
- fig. S1. Structure of gallium.
- fig. S2. Bonding nature of gallium.
- fig. S3. Phonon dispersion of gallenene.
- fig. S4. Effect of number of layers of gallenene b₀₁₀.
- fig. S5. Effect of number of layers of gallenene a₁₀₀.
- fig. S6. Stamping technique used for simultaneous exfoliation of multiple samples.
- fig. S7. AFM analysis.
- fig. S8. Thickness for different substrates.
- fig. S9. Contact angle measurements.
- fig. S10. Gallenene on different substrates.

- fig. S11. Gallenene on Si.
- fig. S12. Gallenene on Si.
- fig. S13. Gallenene on Ag.
- fig. S14. Gallenene on Al.
- fig. S15. Gallenene on Si.
- fig. S16. Gallenene on Ni.
- fig. S17. Gallenene on GaN.
- fig. S18. Band structure of gallenene on different substrates.
- fig. S19. XPS measurements of heterostructures.
- fig. S20. Structure of heterostructure.
- fig. S21. Thermal properties of gallenene.
- fig. S22. Thermal conductivity variation as a function of temperature.
- fig. S23. Defects in gallenene.
- fig. S24. Defects in gallenene.
- fig. S25. Polymorphism.
- fig. S26. Thin film of tin.
- table S1. Contact angle of Ga on different substrates.
- table S2. Structural parameters of the substrate and gallenene.
- References (80–84)

section S1. Bulk gallium structural analysis

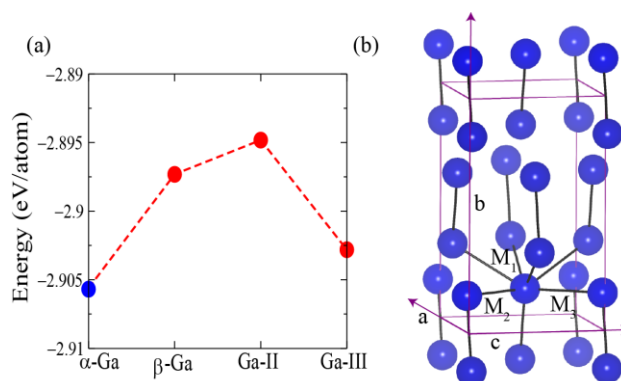


fig. S1. Structure of gallium. (a) The energy per atoms of various bulk Ga structures. (a) Crystal structure of bulk α -Ga, where the unit cell is shown by solid purple color. The lattice parameters are $a = 4.58 \text{ \AA}$, $b = 7.78 \text{ \AA}$, and $c = 4.59 \text{ \AA}$. Each Ga atom has one nearest neighbour, whereas the second (M_1), third (M_2), and fourth (M_3) nearest neighbour of Ga contains two atoms. The calculated Ga-Ga dimer bond length 2.54 \AA . The calculated M_1 , M_2 and M_3 distance are 2.73 \AA (M_1), 2.77 \AA and 2.82 \AA , respectively.

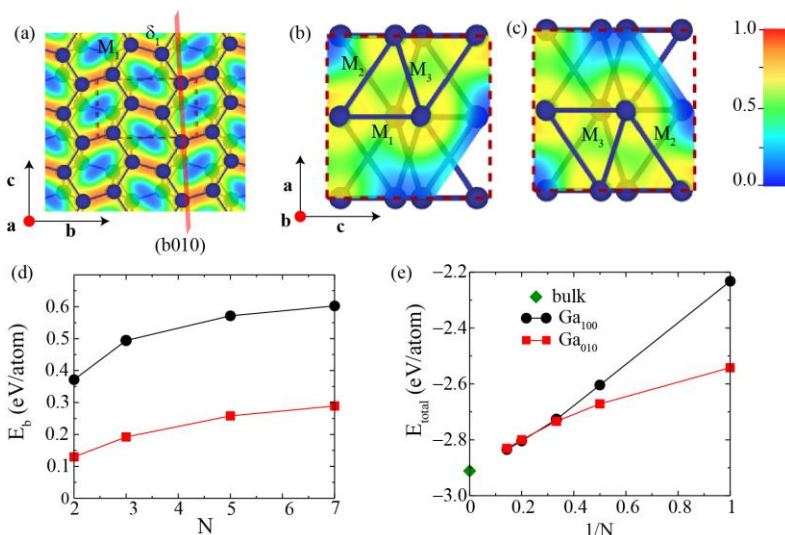


fig. S2. Bonding nature of gallium. (a) Electron localization function (ELF) of Ga bulk structure on bc plane. To identify the bonding nature among the Ga atoms a small tilted plane with respect to ac plane are shown in (b) and (c). The value of ELF 1 and 0.5 corresponding to perfect localization and the electron gas. The electrons are localized between the first nearest neighbour (δ_1) Ga atoms, which indicating covalence bond between the Ga atoms. However, the electrons are less localized (more like uniform distribution) between second (M_1), third (M_2), and fourth (M_3) nearest neighbour bonds. This implies that the second, third, and fourth nearest neighbour bonds are more metallic in nature. This is in good agreement with other findings (80, 81). (d) Interlayer binding energy of a_{100} and b_{010} monolayer structures as function of layer number (N). Interlayer binding energy is off the order of eV per-atom indicating chemical interaction among the layers. (e) Total energy per atom as an inverse function of layer numbers. The interlayer binding and total energy per are calculated using lattice parameters of bulk gallium. The total energy per atom of two different structures of gallene becomes equal above the 3-layers atoms thick, which indicates both are equal energetic to be formed more than 3-layers atomic thick.

section S2. Stability of gallene sheets

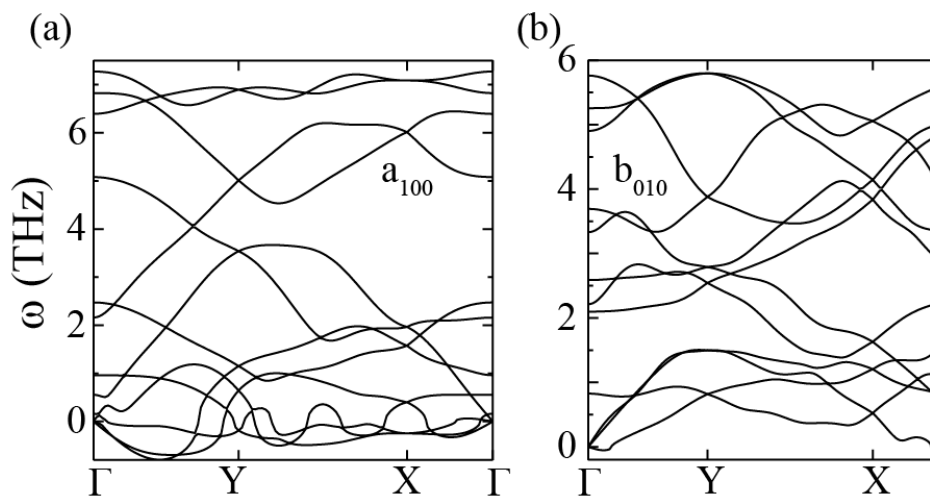


fig. S3. Phonon dispersion of gallene. (a) and (b) are the phonon dispersion of optimized a_{100} and b_{010} monolayer structures. The phonon dispersion of mono layer a_{100} and b_{010} structure are calculated with 96 atoms and 196 atoms of supercell size $4 \times 6 \times 1$ and $7 \times 7 \times 1$ supercell, respectively. The negative values of frequencies are called imaginary frequencies. The modes of imaginary frequency imply that this mode will not be able to produce enough restoring force to keep the structure dynamically stable in free standing form. Thus, the gallene will be dynamically unstable.

section S3. Effect of thickness on the band structure of gallenene

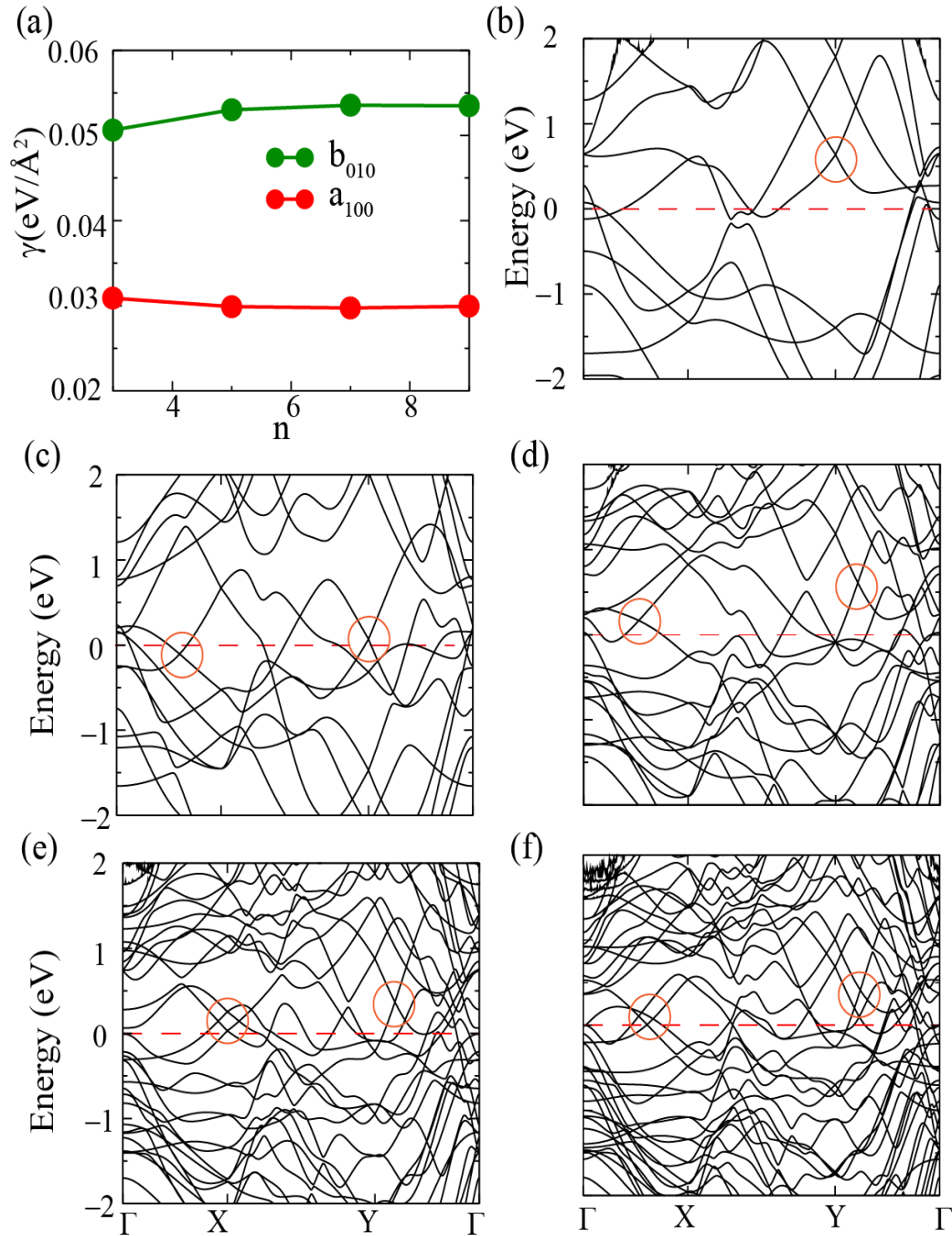


fig. S4. Effect of number of layers of gallenene b_{010} . (a) Surface energy (γ) as a function number of layers (n) for a_{100} and b_{010} gallenene sheets. The surface energy of b_{010} gallenene is higher than that of the a_{100} sheet. The formation of b_{010} surface involves cleaving of relatively stronger covalent bonds, whereas a_{100} surface is formed by cleaving of metallic bonds. Beyond 7 and 5 layers b_{010} and a_{100} respectively, the surface energies become independent of number of layers. (b), (c), (d), (e), and (f) are the electronic band structures of 2L, 3L, 5L, 7L and 9L b_{010} gallenene

sheets. The electronic structures and surface energies are calculated at the bulk lattice parameters. The Fermi energy is set to zero. The bands cross at the Fermi energy (shown by dotted red line) indicating layer independent metallic nature of these sheets. The Dirac like linear dispersion (as shown by orange color circle) is found for all the sheets. The position of Dirac like linear bands change with the number of layers.

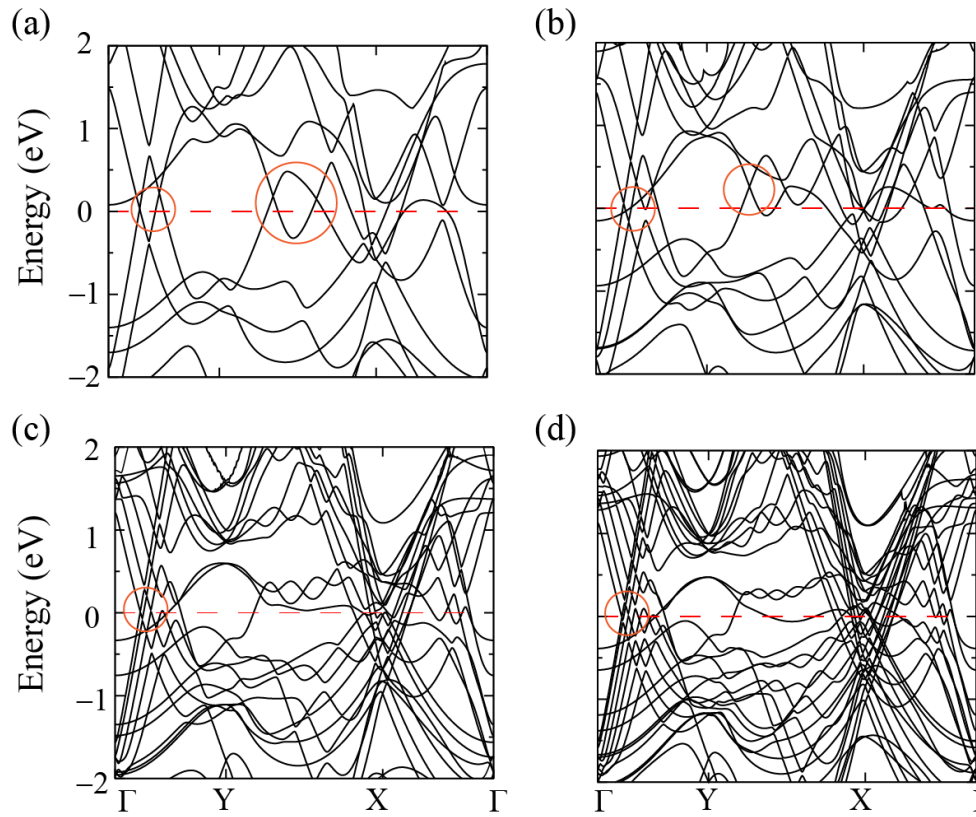


fig. S5. Effect of number of layers of gallene a_{100} . (a), (b), (c), and (d) are the electronic band structure of 2L, 3L, 5L, and 7L of a_{100} gallene sheets respectively. The electronic structure calculations were performed at the bulk lattice parameter. The Fermi energy is set to zero. All the sheets are metallic. The Dirac like linear dispersions (shown by orange color circle) is present in all the structures.

section S4. Stamping technique of solid-melt exfoliation

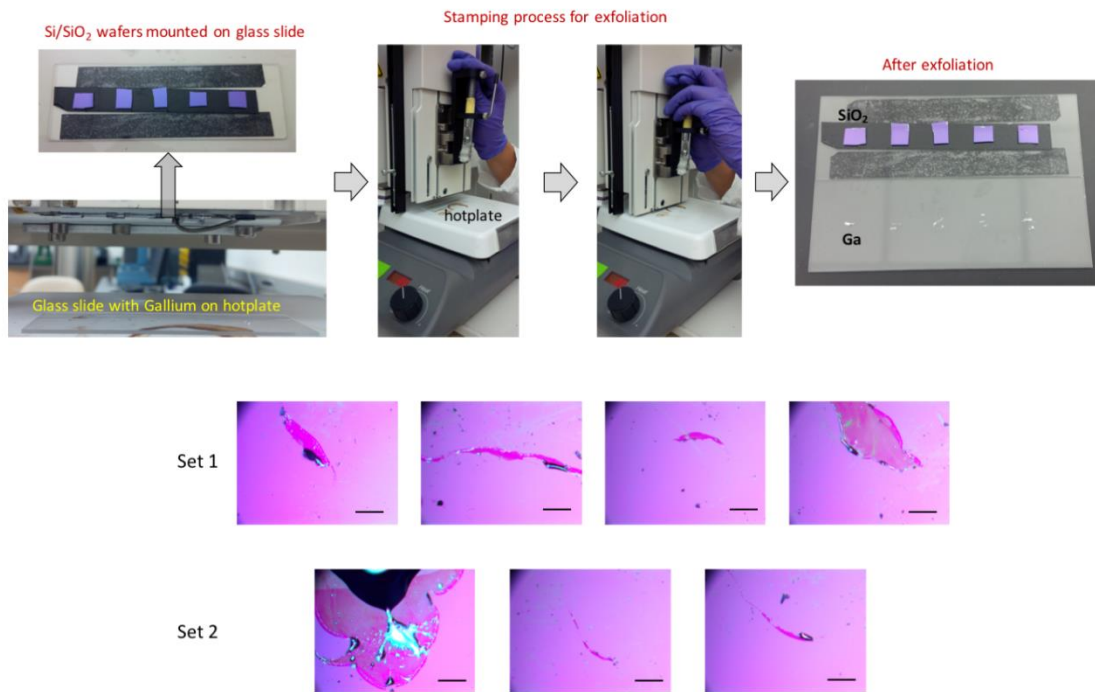


fig. S6. Stamping technique used for simultaneous exfoliation of multiple samples. The Si/SiO₂ wafers (each batch of 5 wafers) were mounted on a glass slide and was then fitted onto the manual stamping arrangement on top of the hotplate. The solid Ga was placed on another glass slide kept directly on the hotplate and heated to temperatures above the melting point of Ga. On subsequent cooling to 300C, the wafers were pressed manually onto the Ga on hotplate and released. Set 1 shows a batch of Si/SiO₂ wafers where 4/5 wafers had Ga films and Set 2 shows a batch with 3/5 wafers with Ga films. In future, we propose to further automate this setup by applying known loads for successful exfoliation of various other low melting point metals.

section S5. AFM analysis of Ga films

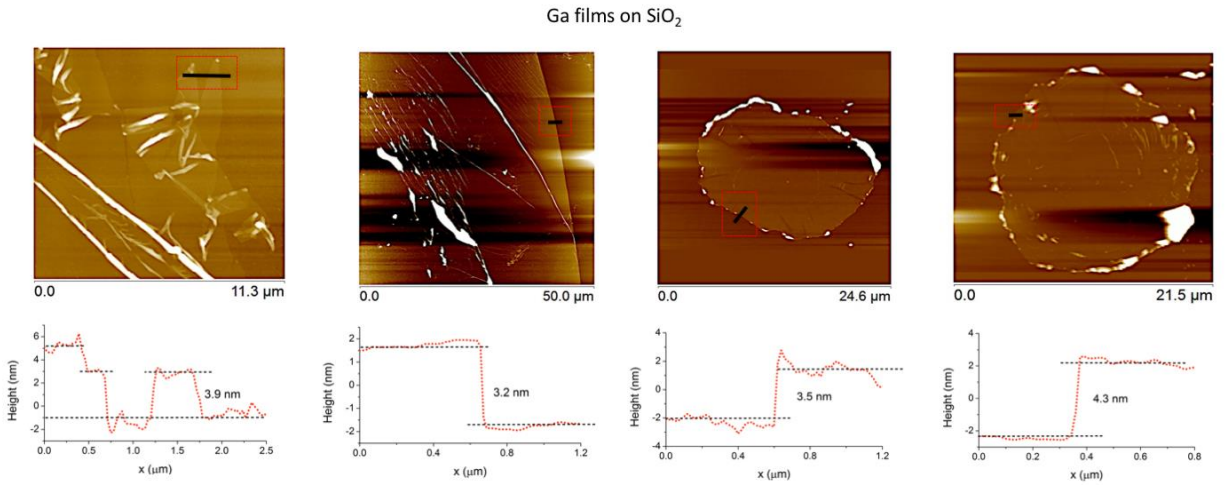


fig. S7. AFM analysis. Representative AFM of Gallenene films of different sizes on SiO₂ showing different thickness.

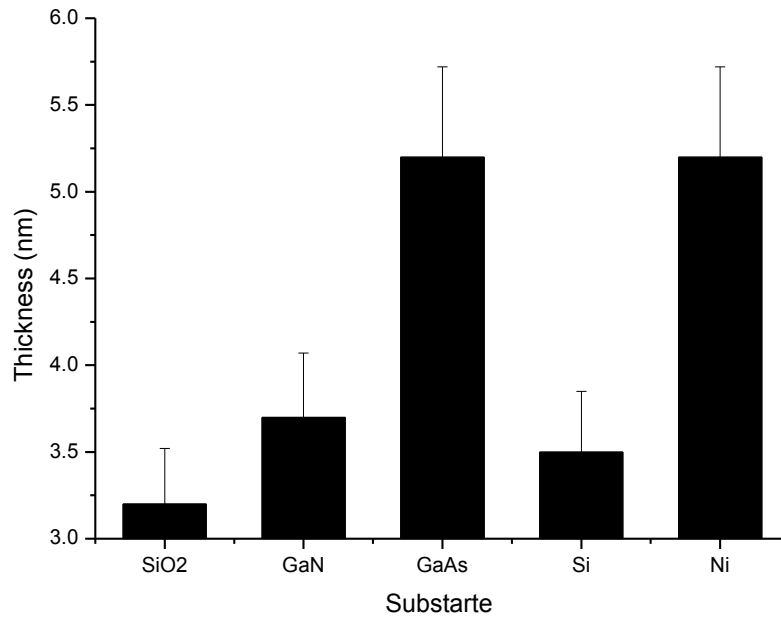


fig. S8. Thickness for different substrates. Comparative plot of thickness of Gallenene exfoliated on different substrate

section S6. Contact angle measurements

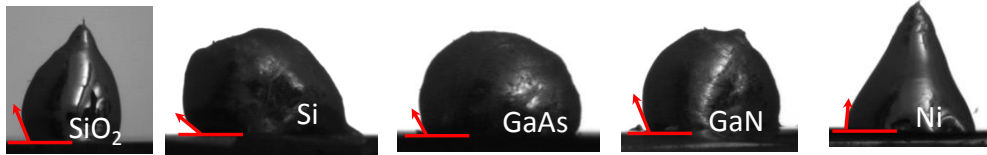


fig. S9. Contact angle measurements. Ga droplet on different substrates and the optical micrographs. The table below shows the contact angle values for Ga on various substrates.

table S1. Contact angle of Ga on different substrates.

Substrate	Contact angle
SiO ₂	70
Si	38
GaAs	58
GaN	67
Ni	91

section S7. Substrate effects on gallenene

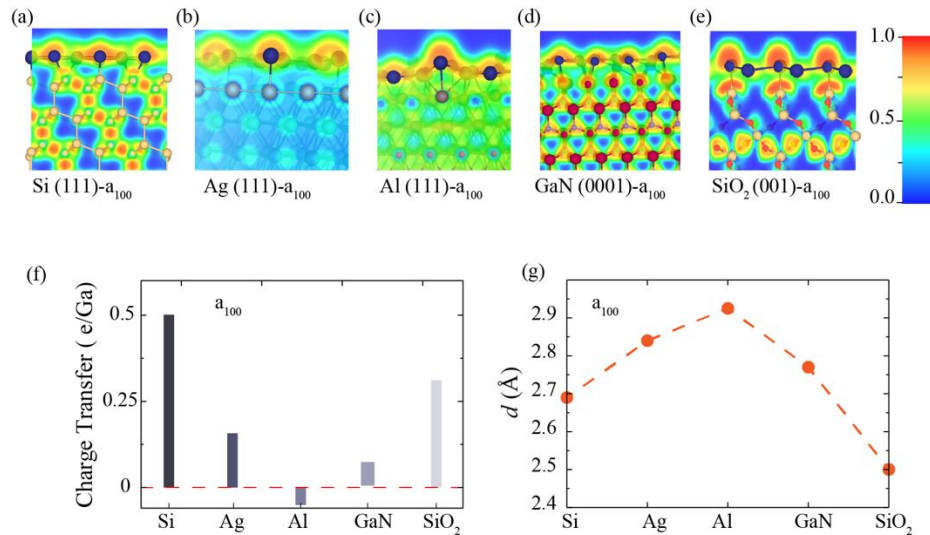


fig. S10. Gallenene on different substrates. (a), (b), (c), (d), and (e) shows electron localization function (ELF) of gallenene a₁₀₀ on Si, Ag, Al, Ga-terminated GaN, and Si-terminated SiO₂ substrate, respectively. (f) Charge transfer between substrate and gallenene a₁₀₀. (g) Average interlayer distance between substrate and gallenene a₁₀₀. Blue, cyan, brown, red, purple and orange colour spheres are symbolized Ga, Si, Ag, Al, Ga (in GaN), N, and O atoms, respectively, otherwise specified. The gallenene structure remains in its original planar form on Si, Ag, and SiO₂ substrates, whereas a small buckling occurs on Al and GaN substrates.

table S2. Structural parameters of the substrate and gallene. Negative and positive sign of strain indicates compressive and tensile strain, respectively.

Substrate	Substrate atomic layer thickness	Gallenene	Cell size		Strain on Gallenene lattice (%)		Remark on gallene stability on the substrate
			substrate	Gallenene	a	b	
Si (111)	4	a ₁₀₀	2×2×1	1×3×1	3.56	1.12	**
		b ₀₁₀	5×3×1	4×4×1	4.11	4.12	*
Si (200)	5	a ₁₀₀	4×4×1	3×5×1	-0.22	1.68	×
		b ₀₁₀	4×5×1	5×6×1	-5.10	-4.88	×
Ag (111)	5	a ₁₀₀	3×3×1	2×2×1	1.3	1.3	**
		b ₀₁₀	4×1×1	5×1×1	1.7	5.94	*
Al (111)	5	a ₁₀₀	3×3×1	2×2×1	1.2	1.2	**
		b ₀₁₀	4×1×1	5×1×1	0.8	3.34	*
α-SiO ₂ (001)	20	a ₁₀₀	1×1×1	1×1×1	15	15	**
	9	b ₀₁₀	1×1×1	2×1×1	5.90	4.59	**
Ni (111)	3	a ₁₀₀	7×7×1	4×4×1	0.08	0.08	*
	5	b ₀₁₀	1×8×1	1×7×1	7.67	2.54	**
GaN (0001)	6	a ₁₀₀	4×4×1	3×3×1	-2.35	-2.35	**

		b ₀₁₀	3×3×1	2×2×1	-3.34	-7.26	*
--	--	------------------	-------	-------	-------	-------	---

(**) Good stability of gallene on the substrate

(*) Do not show good stability on the substrate

(×) Gallene not stable on the substrate

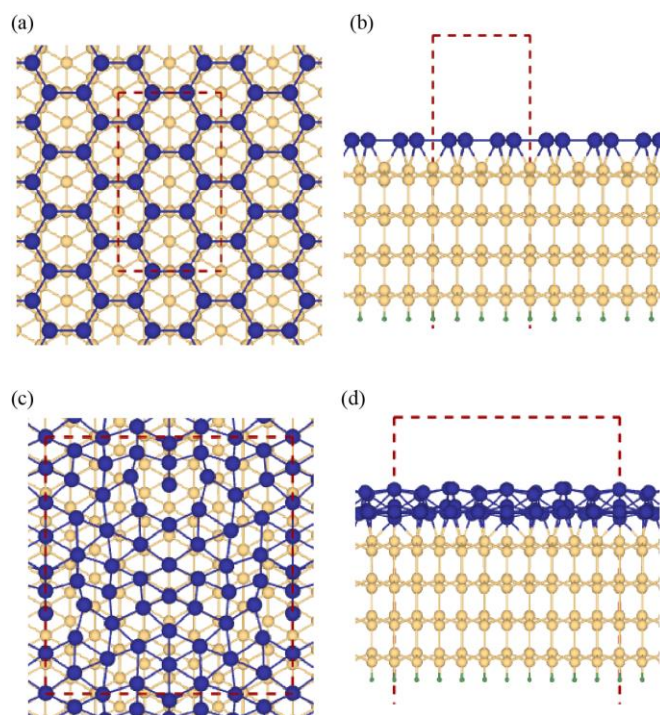


fig. S11. Gallene on Si. (a) and (b) top and side view of gallene a_{100} on 111 surface of Si substrate. (c) and (d) top and side view of gallene b_{010} on (111) surface of Si substrate. The dotted maroon line indicates unit cell of the combined system. The dangling bonds of Si are passivated by H atoms, which are shown in green color spheres.

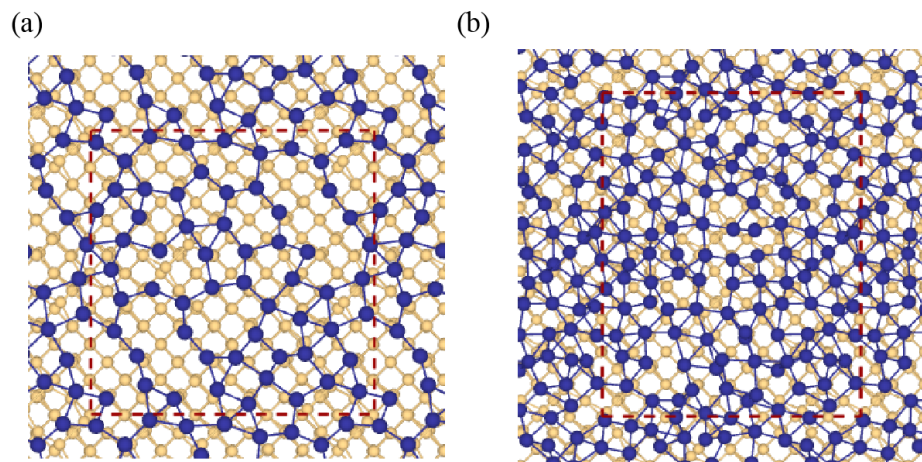


fig. S12. Gallenene on Si. (a) and (b) Top view of gallenene a_{100} and b_{010} structure on (200) surface of Si, respectively. The dotted maroon line indicates unit cell. The dangling bonds of Si are passivated by H atoms.

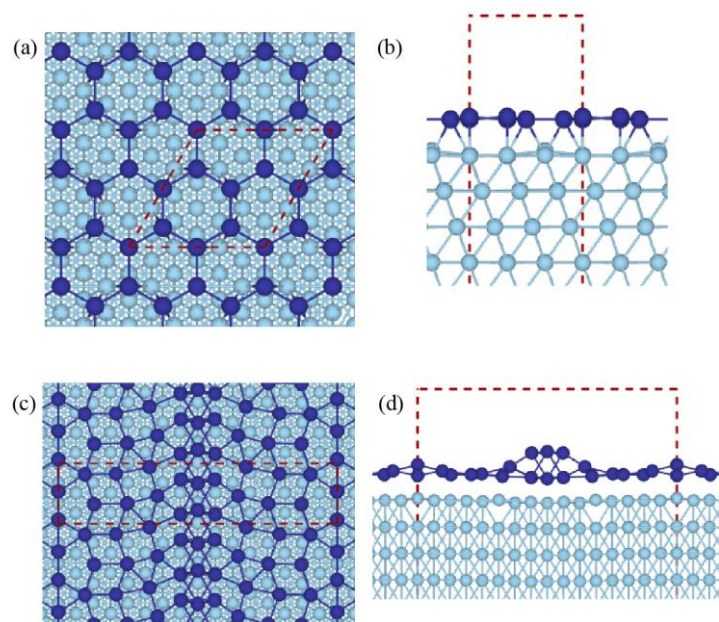


fig. S13. Gallenene on Ag. (a) and (b) top and side view of gallenene a_{100} on (111) surface of Ag substrate. (c) and (d) top and side view of gallenene b_{010} on (111) surface of Ag substrate. The dotted maroon line indicates unit cell.

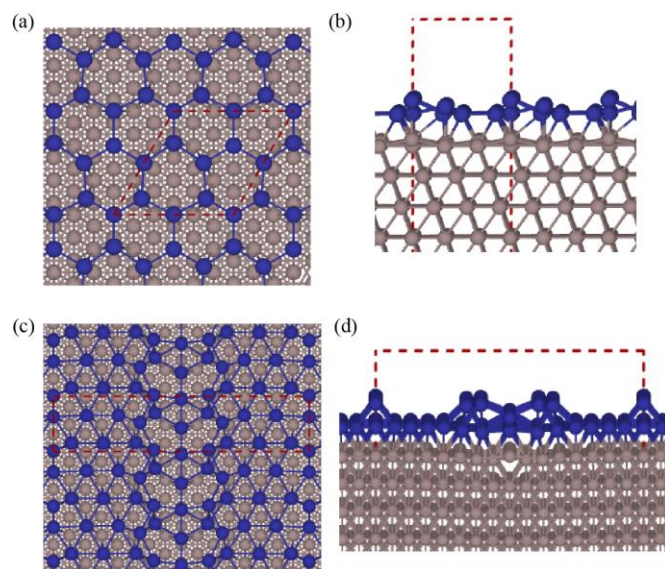


fig. S14. Gallene on Al. (a) and (b) top and side view of gallene a_{100} on (111) surface of Al substrate. (c) and (d) top and side view of gallene b_{010} on (111) surface of Al substrate. The dotted maroon line indicates unit cell.

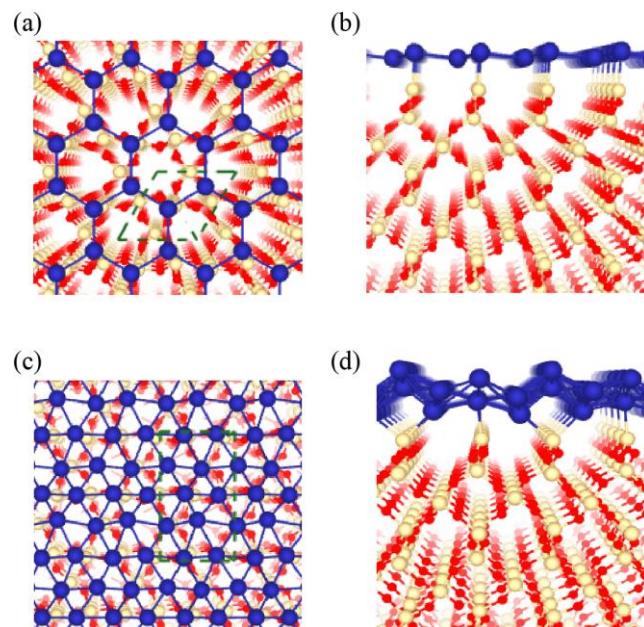


fig. S15. Gallene on Si. (a) and (b) top and side view of gallene a_{100} on Si terminated (0001) surface of α - SiO_2 substrate. (c) and (d) top and side view of gallene b_{010} Si terminated (0001) surface of SiO_2 substrate. O atoms are represented by red color spheres. The dotted green line indicates unit cell of the combined system. The dangling bonds are passivated by H atoms .

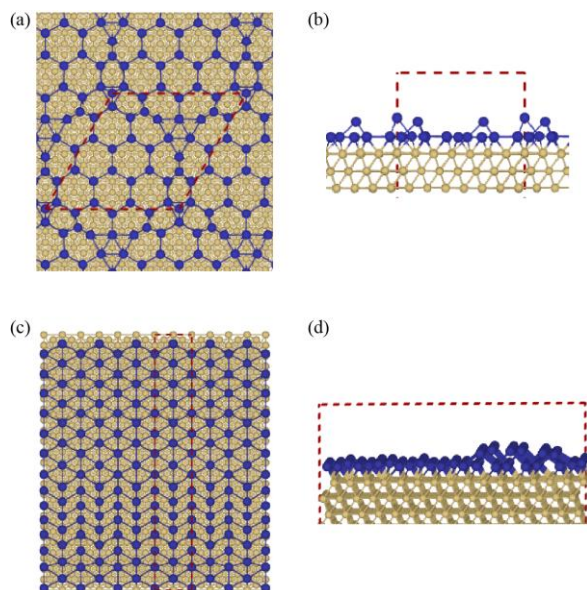


fig. S16. Gallenene on Ni. (a) and (b) top and side view of a_{100} gallenene situated on (111) surface of Ni substrate. (c) and (d) top and side view of b_{010} gallenene located on the (111) surface of Ni substrate. The dotted maroon line indicates unit cell. Yellow colour spheres represent Ni atoms. Due to magnetic and metallic nature, we have set the force convergence criteria and smearing width of 0.3 eV and $< 0.05 \text{ eV/\AA}^2$, respectively. The magnetic properties of gallenene are not explored on Ni substrate.

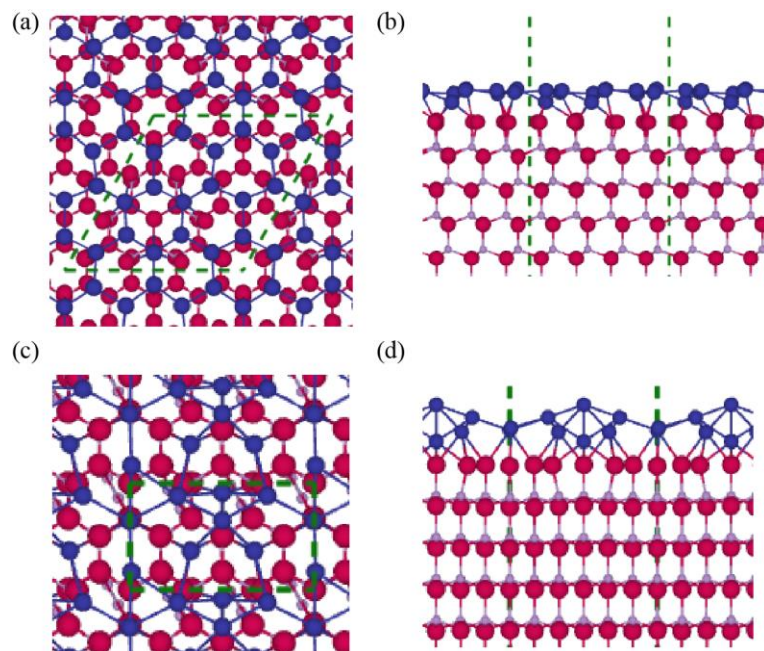


fig. S17. Gallene on GaN. (a) and (b) top and side view of gallene a_{100} on the Ga terminated (0001) surface of GaN substrate . (c) and (d) top and side view of gallene b_{010} situated on the Ga terminated (0001) surface of GaN substrate. The dotted green line indicates unit cell. The force convergence criteria is set to $< 0.02 \text{ eV/\AA}^2$. The first 3-layer of GaN atoms are allowed to relax and rest of the atoms freeze to the bulk atomic position.

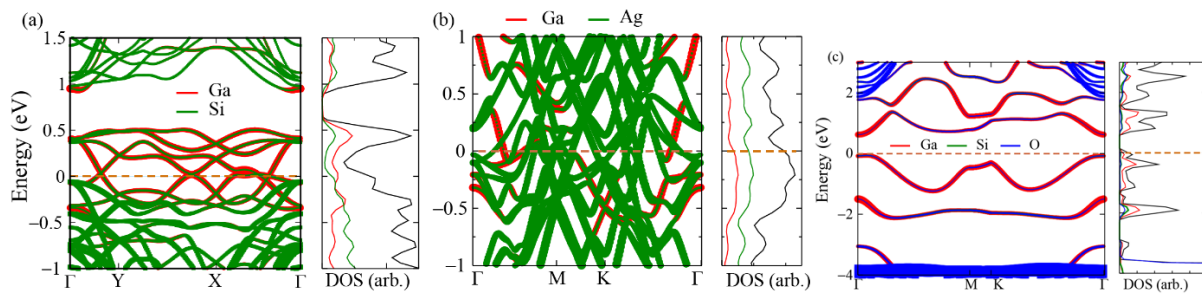


fig. S18. Band structure of gallene on different substrates. (a), (b) and (c) orbitals projected bands structure of gallene (a_{100}) on Si (111) surface, Ag (111) surface and SiO_2 (001) surface. Fermi energy set to zero. The gallene show metallic nature on Si and Ag substrates, whereas gallene show semiconductor nature on SiO_2 substrate. Fermi energy is set to zero and is shown by dotted orange line.

section S8. Absorption measurements on gallene

Measurement details:

To collect spectra on single particles of gallium, standard samples were prepared on SiO₂ and GaAs substrates. These samples were then placed on separate glass coverslips and placed in the beam-path of an inverted optical microscope (Nikon Ti-U) in bright-field mode. Samples were irradiated with a standard halogen lamp, and spectra were collected using a Princeton Instruments spectrometer (Isoplane 320) and camera (ProEM-HS). With this instrument setup, it is possible to measure the absorbance of samples across the visible range and down to 350 nm. Thin layers of gallium appeared blue in the microscope and were easily found on both substrates. Thicker layers of gallium have a purple appearance, and they were only observed on the sample prepared on the SiO₂ substrate. The actual absorbance values were determined by comparing the signal intensity through the sample area against the intensity through background areas.

section S9. XPS measurements on Ga/MoS₂ heterostructures

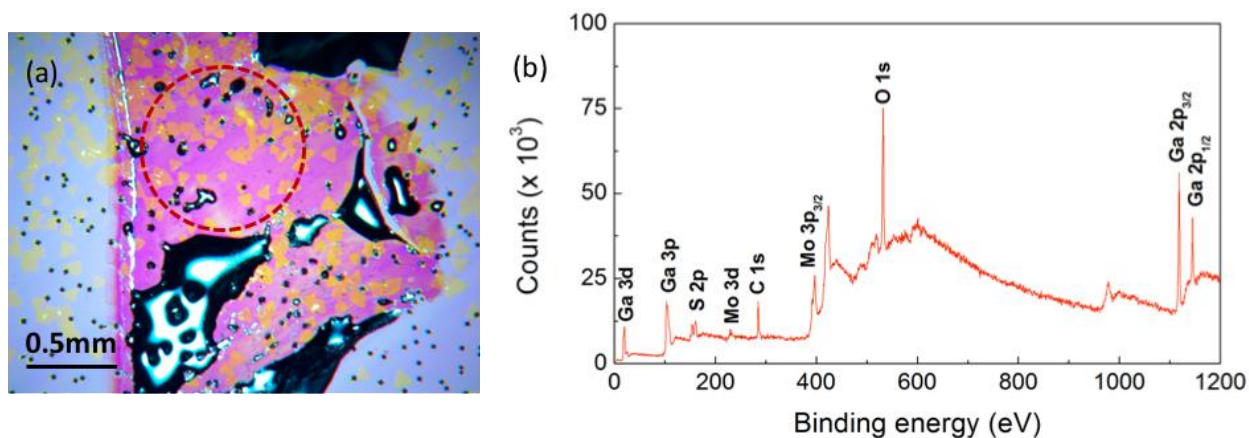


fig. S19. XPS measurements of heterostructures. (a) Optical micrograph of a large area gallene on top of MoS₂ flakes. XPS measurements were done in the region outlined in red. (b) Survey scan showing the Mo, S, Ga peaks.

Additional details: Ga 3s BE = 161 eV Ga₂O₃ Ga 3s BE = 160.7 eV Ga and Ga₂O₃ has 3p_{3/2} around 105 eV. Ga₂S₃ 3p_{3/2} 106.6 eV. GaS 3p_{3/2} 105.3 eV GaS 3p_{1/2} at 108.7 eV. Ga₂O₃ 3d at 20 eV SiO₂ Si 2p_{3/2} at 103 eV.

section S10. Structural stability of Ga/MoS₂ heterostructures

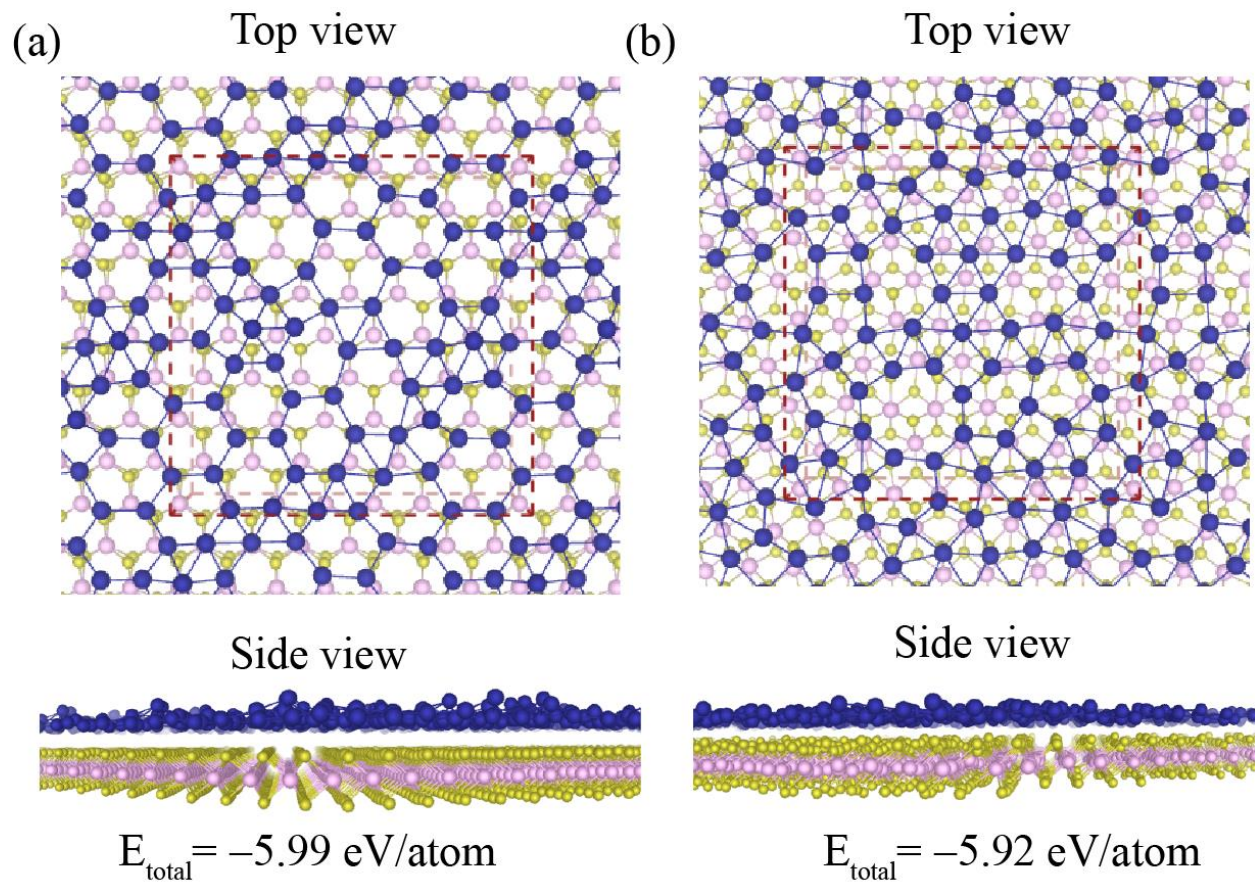


fig. S20. Structure of heterostructure. (a) Top view and side view of 2D Ga on top of MoS₂

section S11. Thermal conductivity of gallenene

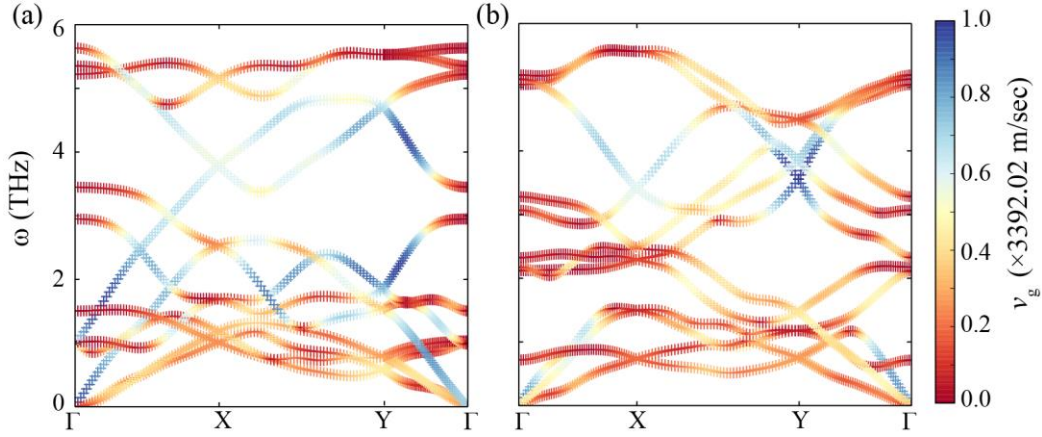


fig. S21. Thermal properties of gallenene. (a) and (b) phonon group velocity along the symmetric line in the 1st Brillouin zone of a_{100} and b_{010} at strain value of 6% and 2%, respectively. The group velocity of acoustic modes (ZA, LA and TA) of gallenene are significantly lowered compared to the other 2D sheets such as graphene¹⁹ ($v_{LA} = 21400 \text{ ms}^{-1}$ and $v_{TA} = 14200 \text{ ms}^{-1}$), silicene²⁰ ($v_{LA} = 6400 \text{ ms}^{-1}$ and $v_{TA} = 3700 \text{ ms}^{-1}$), germanene²¹ ($v_{LA} = 4031 \text{ ms}^{-1}$ and $v_{TA} = 2124 \text{ ms}^{-1}$), and stanene²¹ (ac direction (3388 ms^{-1} and 868 ms^{-1}) and ZZ (3366 ms^{-1} and 833 ms^{-1})). Thermal conductivity is proportional to the square of the group velocity indicating low thermal conductivity of gallenene.

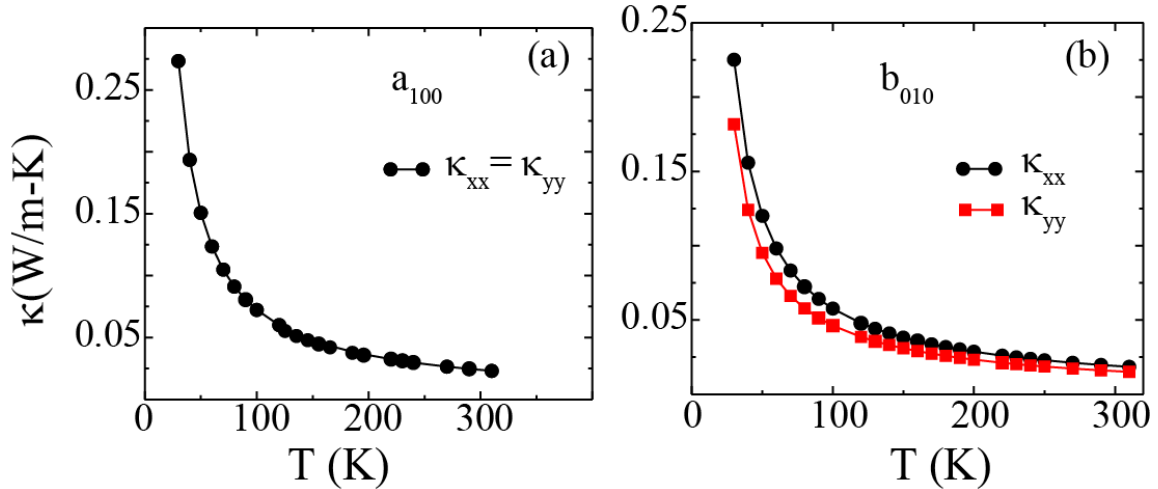


fig. S22. Thermal conductivity variation as a function of temperature. (a) and (b) lattice thermal conductivity of 6% and 2% strained a_{100} and b_{010} gallenene, respectively as function of absolute temperature.

section S12. Defects in gallenene

Mono-vacancy gallenene

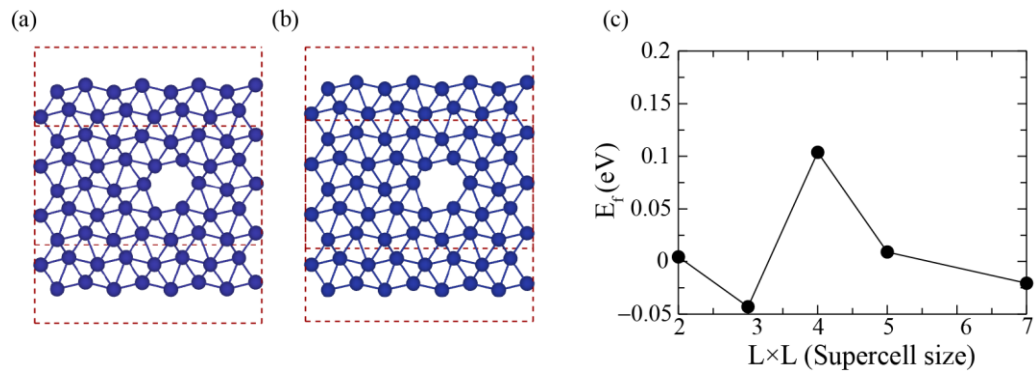


fig. S23. Defects in gallenene. (a) and (b) shows unrelaxed and relaxed structures of mono-vacancy b_{010} gallenene. The Ga atoms at the vacancy site does not show much relax from their original position. The change in bond length between Ga-Ga at the vacancy site is $\sim 0.1-0.2\text{\AA}$. (c) Formation energy of the mono-vacancy as function of cell size. The energy of removing Ga atoms is low indicating formation of vacancy in experimental growth of gallenene.

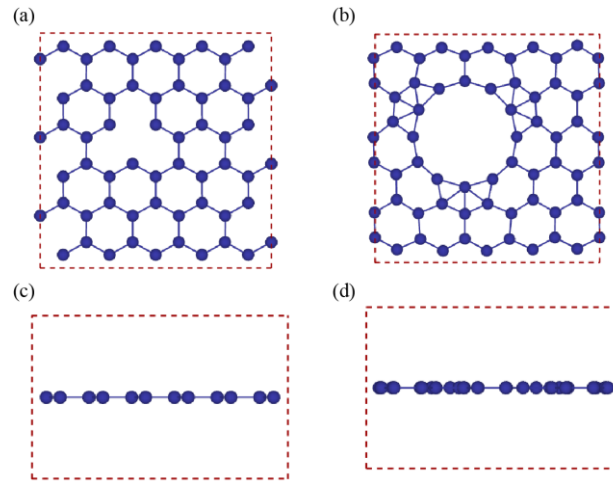


fig. S24. Defects in gallenene. (a) and (b) shows top view of unrelaxed and relaxed structure of mono-vacancy a_{100} gallenene. (c) and (d) shows side view of the unrelaxed and relaxed structure of mono-vacancy a_{100} gallenene. The mono-vacancy structure gets reconstructed and formed new kind of sheet indicating vacancy can create newer reconstructed gallenene structure. The supercell size $3 \times 5 \times 1$ is considered for mono-vacancy study. The spin polarization calculations of mono-vacancy gallenene do not show any magnetic ordering indicating mono-vacancy gallenene will be non-magnetic.

section S13. Polymorphism in gallenene Borophene inspired Gallenene

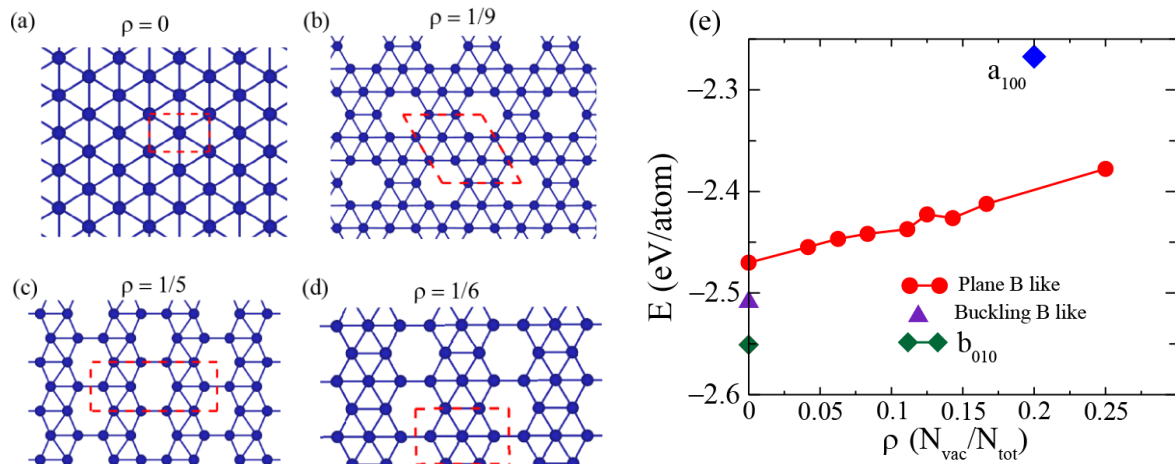


fig. S25. Polymorphism. (a), (b), (c) and (d) show borophene like gallenene structures, which are known to be stable Borophene structure (82-84) (e) Total energy per atom as function of vacancy concentration (ρ). The collinear spin polarization calculations do not show any magnetic ordering, which indicates these sheets will be non-magnetic.

section S14. Exfoliation of ultrathin Sn sheets

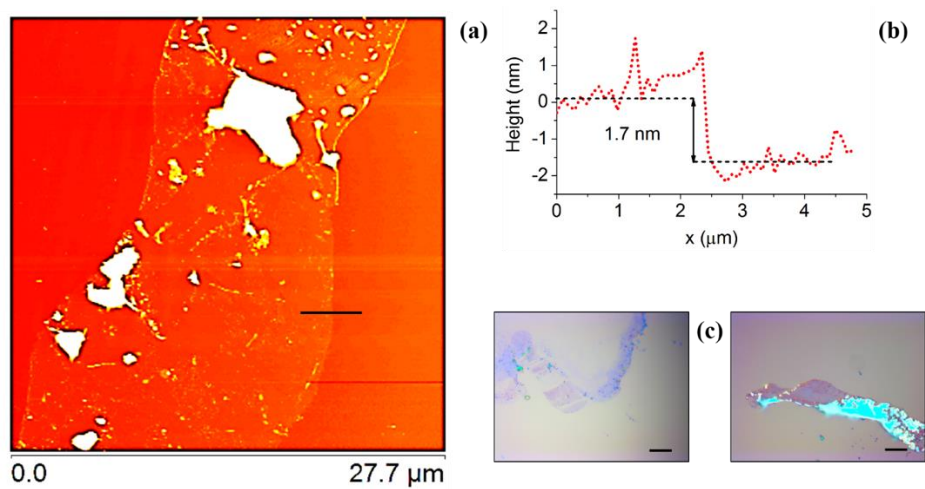


fig. S26. Thin film of tin. (a) 2D AFM image of tin (Sn) exfoliated using current technique. (b) Line profile of AFM edge as marked as line in (a). (c) optical image of the thin sheet of tin.